

# Seismic assessment of existing precast structures with dry-friction beam-to-column joints

Andrea Titi<sup>1</sup>  · Fabio Biondini<sup>1</sup>  · Giandomenico Toniolo<sup>1</sup>

Received: 26 January 2017 / Accepted: 18 November 2017 / Published online: 4 December 2017  
© Springer Science+Business Media B.V., part of Springer Nature 2017

**Abstract** In seismic countries of Southern Europe, including Italy, a large stock of existing precast structures for industrial buildings is characterized by beam-to-column dry friction joints. Several failures of this type of structures occurred during recent seismic events, including the Emilia earthquakes in 2012, due to the loss of the friction restraint and shift of the beam out of the support at the top of the column under the combined effects of horizontal and vertical seismic shaking. The seismic behaviour of precast structures with dry-friction joints is investigated based on nonlinear dynamic analysis to support the vulnerability assessment and design of seismic retrofitting interventions of existing industrial buildings. A dry-friction modelling of beam-to-column joints is proposed and case studies are presented to identify the most critical factors affecting the seismic response of precast frame buildings. The results show that flexible systems are more prone to structural failure due to the loss of support of the beam, particularly when the frequency content of the main shock of the seismic excitation includes the natural frequency of the structure in the vertical direction.

**Keywords** Precast buildings · Existing structures · Dry-friction joints · Seismic vulnerability

## 1 Introduction

In Italy and other seismic countries of Southern Europe, precast concrete buildings for commercial and industrial use are quite widespread. They consist of one-story or multi-story structures (generally limited to two or three floors) and, particularly for industrial use, most of them have hinged beam-to-column connections (Biondini et al. 2010). The

---

✉ Andrea Titi  
andrea.titi@polimi.it

<sup>1</sup> Department of Civil and Environmental Engineering, Politecnico di Milano, Piazza Leonardo da Vinci 32, 20133 Milan, Italy

dissipative zones are located at the base of the columns, where plastic hinges are expected to develop when strong earthquakes occur. Extensive theoretical and experimental research demonstrated that precast structures, based on a proper capacity design of connections, could achieve the same seismic performance of cast-in-place structures in terms of global strength and ductility (Biondini and Toniolo 2009). The role of the connections among different components in precast structures have been also investigated within recent European research projects, including SAFECAST (Toniolo 2012) and SAFECLADDING (Colombo et al. 2014). Pseudo-dynamic tests on a full-scale multi-story building have been carried out within SAFECAST to study the seismic performance of the structure for different arrangements of the beam-to-columns joints (Negro et al. 2013). Moreover, linear and nonlinear dynamic analyses demonstrated the fundamental role of a proper modelling of the connections to reproduce the seismic response of the structure (Biondini et al. 2012). The main purpose of the SAFECLADDING research program was to investigate the role of cladding wall panel connections on the seismic performance of precast structures by means of a large experimental campaign (Dal Lago et al. 2017; Negro and Lamperti Tornaghi 2017), since recent seismic events highlighted the inadequacy of the current design approach for panel fastening systems (Biondini et al. 2013a). This was confirmed by the significant number of panel-to-structure connection failures occurred during the 2009 L'Aquila earthquake in Italy (Toniolo and Colombo 2012).

However, despite the significant progresses in this field, a large stock of existing precast buildings is characterized by high seismic vulnerability due to lack of proper seismic detailing. In particular, beam-to-column connections are usually simple supports designed to transfer shear due to gravity loads by friction only. For this type of structures, the combination of horizontal and vertical components of the seismic motion may lead to exceed the strength provided by friction and, consequently, to lose the support of the beam. The impact of this type of structural failure can be dramatic, as shown by the seismic events which struck the Emilia Romagna region in Italy in 2012 causing 27 casualties, thousands of homeless people and severe direct and indirect economic losses for almost €6B (Magliulo et al. 2014). A significant number of structural collapses occurred during the Emilia earthquakes is indeed ascribable to the use of dry friction beam-to-column joints allowed by the non-seismic code provisions in force at the construction time (Fig. 1).

A detailed description of the seismic performance of precast buildings and an overview of the damages caused by the Emilia earthquakes can be found in Liberatore et al. (2013), Belleri et al. (2015a), Bourmas et al. (2014) and Magliulo et al. (2014). Based on the data provided by the Italian National Institute of Statistics (ISTAT) on building stock's age of construction and considering the evolution of the seismic classification of Emilia region, Manfredi et al. (2014) described and applied a damage assessment procedure to infilled RC buildings. Artioli et al. (2013) described the effects of the Emilia earthquakes on industrial facilities dating back to the early twentieth century, such as chimneys and dewatering facilities. Babič and Dolšek (2016) investigated the impact of structural components on fragility curves of single-story precast industrial buildings. Casotto et al. (2015) developed a seismic fragility model for Italian RC precast buildings, to be used in earthquake loss estimation and seismic risk assessment. Finally, Braga et al. (2014) described a procedure to speedup the post-earthquake community recovery, since Emilia earthquakes hit a highly industrialized area.

This paper presents a procedure for seismic assessment of existing precast frame buildings based on a proper modelling of the beam-to-column friction joints. Nonlinear time-history analyses under simultaneous horizontal and vertical components of the seismic excitation are performed to simulate the structural collapse due to loss of support of the beam, with emphasis on the seismic response and structural performance under the



**Fig. 1** Structural collapse of a precast building occurred during the Emilia earthquake (May 2012) due to loss of support of the roof beam

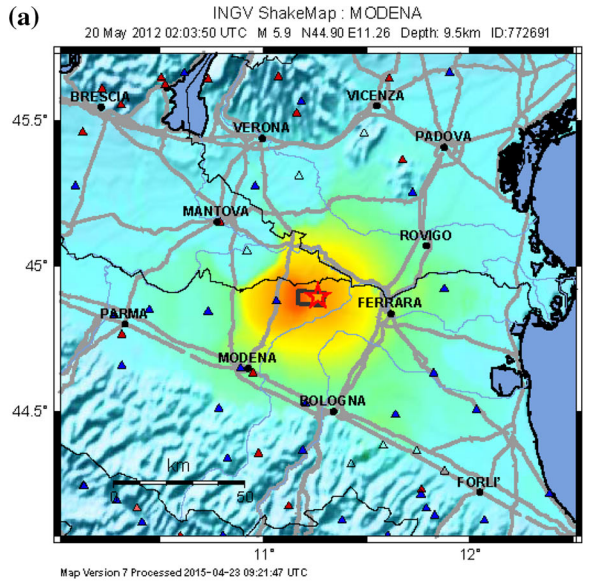
Emilia earthquakes. In particular, the influence of the neoprene-concrete friction coefficient on the seismic response of precast frame buildings is investigated. The results are finally discussed to show the importance of a proper modelling of the hysteretic behavior of dry-friction joints for seismic vulnerability assessment and design of retrofitting interventions of existing precast buildings in seismic areas.

## 2 Emilia earthquakes

On May 2012, a sequence of seismic events struck the Emilia region in Northern Italy. The two main events occurred on May 20th and May 29th with moment magnitude  $M_w$  equal to 5.8 and 5.6, respectively (source: <http://www.ingv.it>). The affected area was characterized by a high number of industrial buildings, mainly one-story structures with few or no seismic provisions, since the seismicity of the territory has been codified in 2003 (Liberatore et al. 2013; Manfredi et al. 2014) and actually applied in design since 2015.

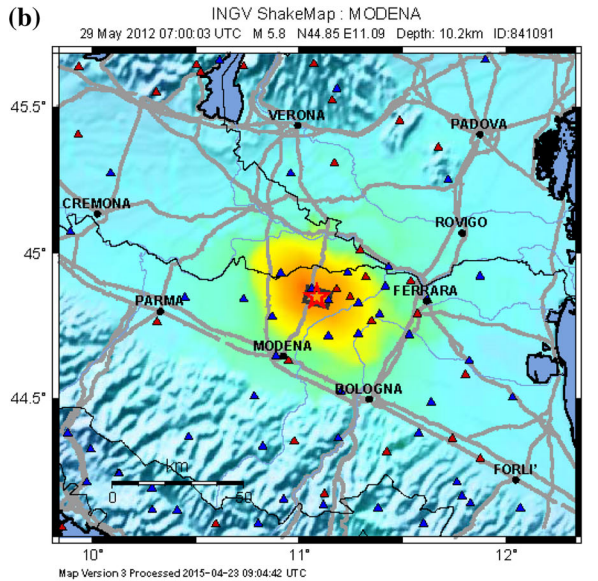
A summary of the peak and integral intensity measures for different stations within an epicentral distance < 50 km can be found in Iervolino et al. (2012). Figure 2 shows the maps of ground shaking associated to peak ground acceleration (PGA), peak ground velocity and instrumentally derived intensity for the two events (Lauciani et al. 2012). The ground motion derived intensity shakemaps are determined using the conversion relations between ground motion parameters and Mercalli–Cancani–Sieberg (MCS) intensity scale proposed by Faenza and Michelini (2010, 2011). These maps indicate a potential damage from moderate to heavy. A series of accelerometer stations within the Italian Strong Motion Network (RAN—Rete Accelerometrica Nazionale) were installed in the affected area. Figures 3 and 4 show the horizontal (N–S and E–W) and vertical (Z) components of the acceleration recorded at the station of Mirandola (MRN), the closest to the epicenter. For both events, the PGA in the horizontal direction is about 0.30 g. Considering the hazard curve of the site shown in Fig. 5 in terms of mean annual rate of exceedance, the

**Fig. 2** Shaking maps of the Emilia earthquakes: **a** May 20th, 2012; **b** May 29th, 2012. Source <http://shakemap.rm.ingv.it>; Last access: October 2016



PERCEIVED SHAKING	Not felt	Weak	Light	Moderate	Strong	Very strong	Severe	Violent	Extreme
POTENTIAL DAMAGE	none	none	none	Very light	Light	Moderate	Mod./Heavy	Heavy	Very Heavy
PEAK ACC.(mg)	<0.05	0.3	2.8	6.2	12	22	40	75	>139
PEAK VEL.(cm/s)	<0.02	0.1	1.4	4.7	9.6	20	41	86	>178
INSTRUMENTAL INTENSITY	I	II-III	IV	V	VI	VII	VIII	IX	X+

Scale based upon Walden et al. (2012)



PERCEIVED SHAKING	Not felt	Weak	Light	Moderate	Strong	Very strong	Severe	Violent	Extreme
POTENTIAL DAMAGE	none	none	none	Very light	Light	Moderate	Mod./Heavy	Heavy	Very Heavy
PEAK ACC.(mg)	<0.05	0.3	2.8	6.2	12	22	40	75	>139
PEAK VEL.(cm/s)	<0.02	0.1	1.4	4.7	9.6	20	41	86	>178
INSTRUMENTAL INTENSITY	I	II-III	IV	V	VI	VII	VIII	IX	X+

Scale based upon Walden et al. (2012)

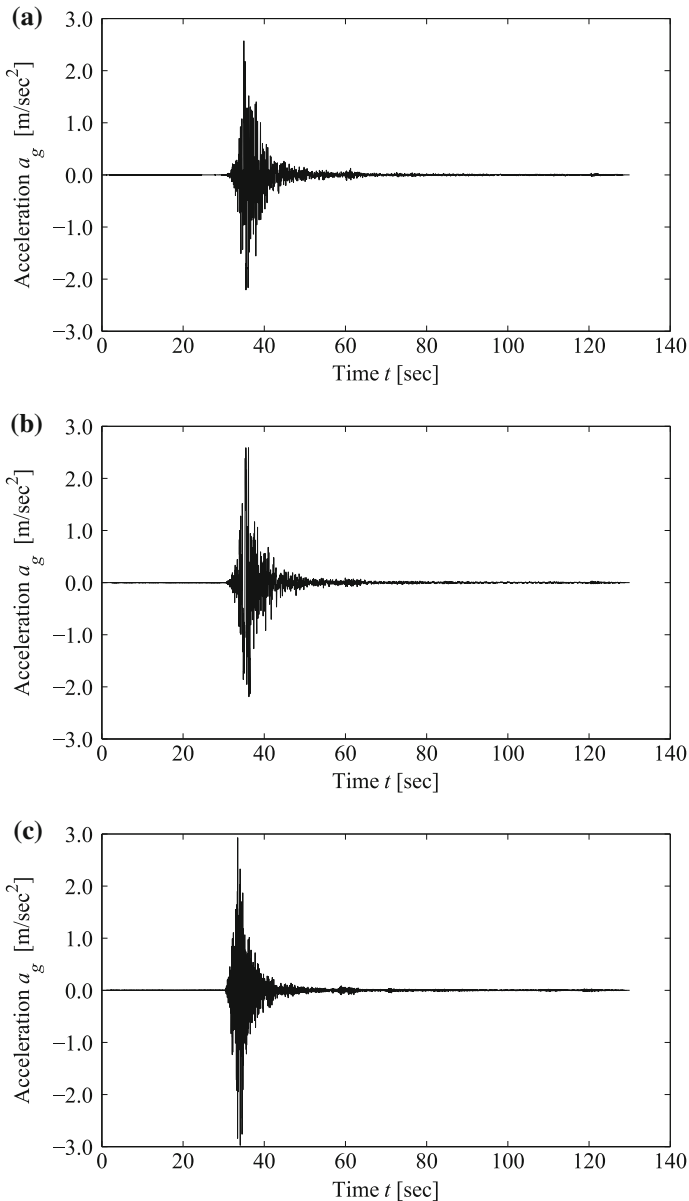


**Fig. 3** Strong ground motion recordings at Mirandola station, MO, Italy, May 20th, 2012, 02:03:52 (UTC). **a** E–W, **b** N–S, **c** Vertical (Z). *Source:* Italian Civil Protection Department

registered PGA is a bit higher than the seismic intensity related to a return period  $T_r = 2475$  years. Consequently, also the recorded spectra at MRN station are comparable or greater than the corresponding uniform hazard spectra. However, the probabilistic estimation did not underestimate the hazard in the area since the other nearby stations experienced response spectra that were generally much below the design spectra (Iervolino et al. 2012).

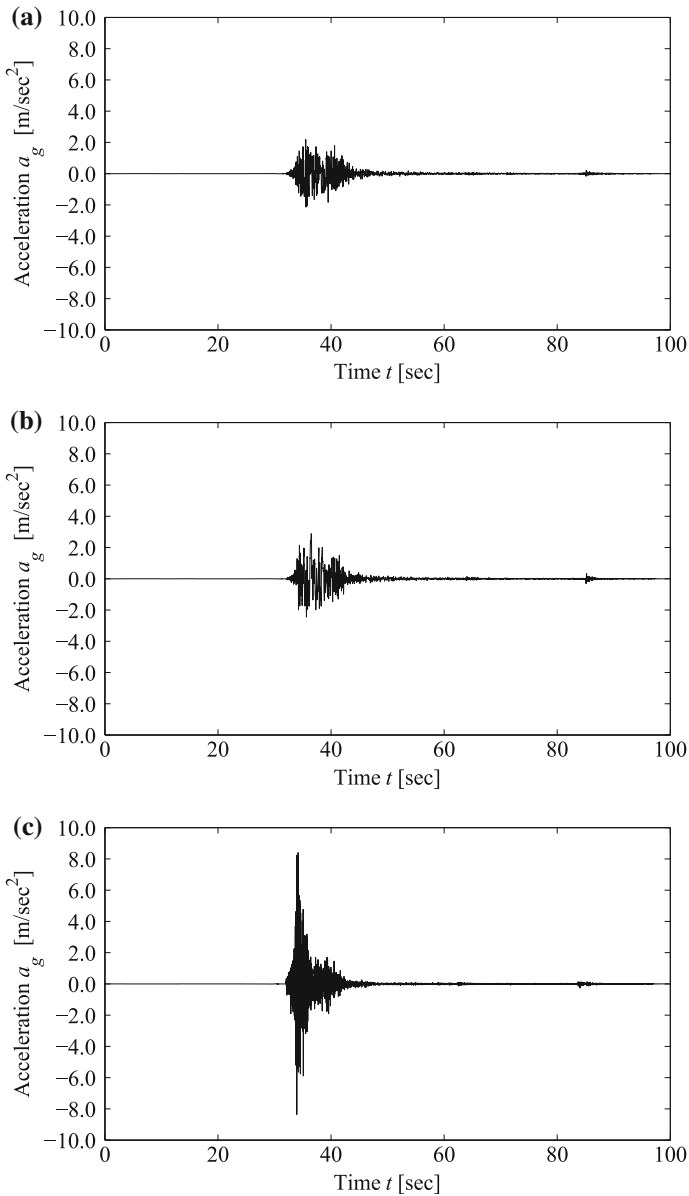


**Fig. 4** Strong ground motion recordings at Mirandola station, MO, Italy, May 29th, 2012, 07:00:03 (UTC). **a** E–W, **b** N–S, **c** Vertical (Z). *Source:* Italian Civil Protection Department

It is worth mentioning that the peculiarity of the Emilia seismic events was a very strong vertical component of the motion, in particular for the event of May 29th. As shown in Fig. 4c, the vertical PGA is almost three times higher than the horizontal PGA. This difference is clearly highlighted by the corresponding response spectra shown in Fig. 6. The peak values are associated with the lower vibration periods (about 0.2 s) that are in the range of the typical natural vibration periods in the vertical direction of precast buildings,

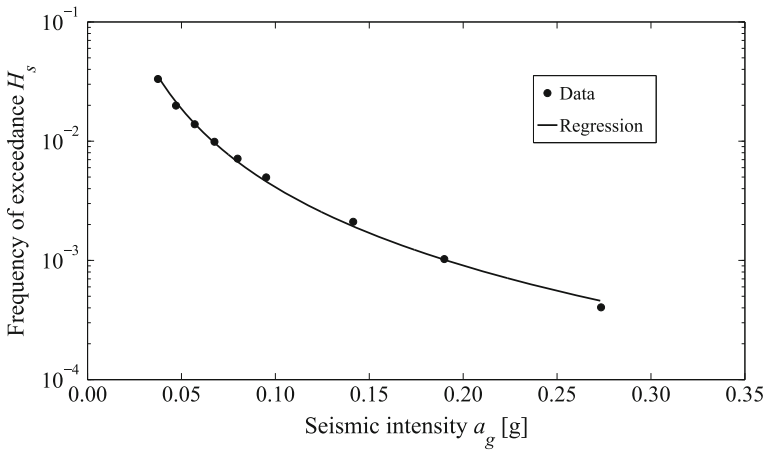


**Fig. 5** Hazard curve for the site of Mirandola, MO, Italy

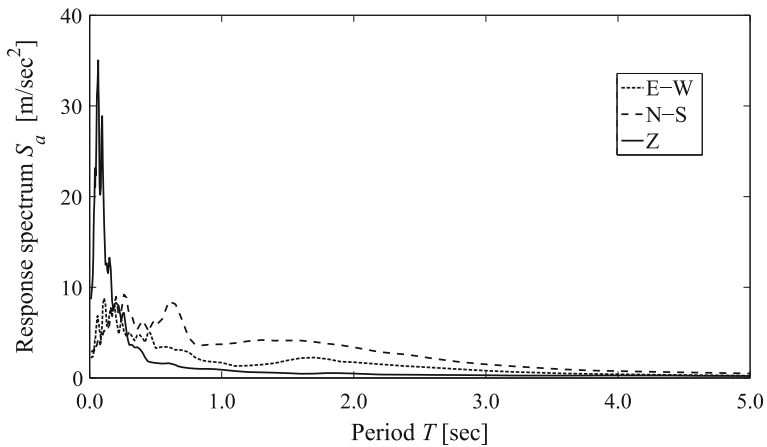


**Fig. 6** Response spectra at Mirandola station, MO, Italy, for the event recorded on May 29th, 2012. *Source:* Italian Civil Protection Department

whereas the period in the horizontal direction may generally range between 0.8 and 1.4 s (Olgiati et al. 2011). Therefore, the combination of horizontal and vertical ground motions, together with the lack of appropriate seismic provisions, was one of the primary reasons of the significant number of structural collapses of precast buildings due to the loss of support of the main beams.

### 3 Friction modelling

In many precast industrial buildings, the strength of the beam-to-column joints is provided only by friction between the two surfaces in contact, for example concrete and neoprene. The corresponding maximum shear capacity can be described by Coulomb’s law of dry

friction. In the following, the criteria adopted for modelling the behaviour of dry-friction beam-to-column joints are briefly presented.

### 3.1 Single degree of freedom system with dry friction

According to the Coulomb’s law of dry friction, the force required to produce sliding between two bodies in contact is proportional to the normal compression force acting in the plane of contact. With reference to the spring–mass single degree of freedom (SDOF) system with dry friction shown in Fig. 7, the friction force  $H$  can be evaluated as follows:

$$H = \mu N = \mu W \tag{1}$$

where  $N$  is the normal force associated with the weight  $W = mg$  of the mass  $m$ , and  $\mu$  is the friction coefficient. The friction force resists the motion depending on the direction of the velocity (Chopra 2007; Rao 2011).

*Case 1 Motion with  $\dot{x} > 0$  (Fig. 7b)*

The equation of motion can be derived as follows:

$$m\ddot{x} + kx = -H(t) = -\mu N \tag{2}$$

which is a second order nonhomogeneous differential equation. The solution is:

$$x(t) = A_1 \cos \omega_n t + A_2 \sin \omega_n t - \frac{\mu N}{k} \tag{3}$$

where  $\omega_n = \sqrt{k/m}$  is the natural frequency of vibration,  $\mu N/k$  is the static displacement of the spring under the friction force  $H$ ,  $A_1$  and  $A_2$  are constants depending on the boundary conditions.

*Case 2 Motion with  $\dot{x} < 0$  (Fig. 7c)*

The equation of motion can be derived as follows:

$$m\ddot{x} + kx = H(t) = \mu N \tag{4}$$

The solution has the same form as for Case 1, with a different sign of the particular integral:

$$x(t) = A_3 \cos \omega_n t + A_4 \sin \omega_n t + \frac{\mu N}{k} \tag{5}$$

These solutions show that in each half cycle the motion is harmonic, with the static equilibrium position changing from  $+\mu N/k$  to  $-\mu N/k$  at each half cycle. The response of a Coulomb friction oscillator subjected to harmonic loads and base excitations is shown in Hong and Liu (2000). More details can be found in Rao (2011).

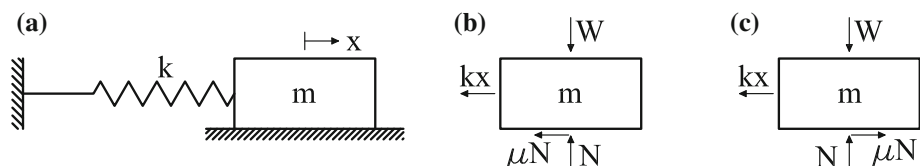


**Fig. 7** Spring-mass single degree of freedom system (SDOF) with Coulomb dry-friction



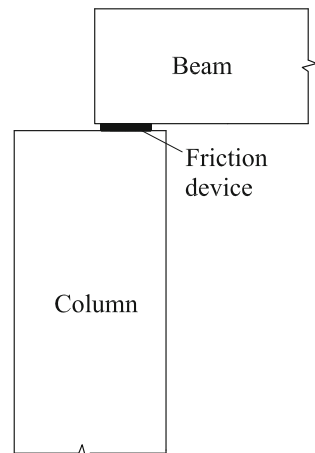
### 3.2 Numerical modelling of dry-friction connections

The numerical modelling is based on the flat slider bearing element available in the OpenSees library (Mazzoni et al. 2006). This element is defined by two nodes, one associated with the flat sliding surface and one related to the slider. The element can have zero length or the appropriate bearing length. For the analysis of two-dimensional systems, the bearing has uniaxial elastic and friction properties for shear deformations, with elastic stiffness  $K_t$  and friction coefficient  $\mu$ , and uniaxial properties for normal deformations and rotations, with elastic stiffness  $K_n$  and  $K_\phi$ , respectively.

The flat slider bearing element is adopted as friction device to represent the beam to column dry connection, as shown in Fig. 8. In this paper, Coulomb friction with constant friction coefficient is considered. However, it is worth noting that this kind of modelling can also accommodate friction coefficients varying during the seismic motion depending on the sliding velocity, axial pressure and temperature at the sliding surface (Kumar et al. 2015). The stiffness of the connection device can be evaluated considering the elastic deformation of the neoprene pad and type of sliding surface, e.g. concrete-neoprene (Magliulo et al. 2008). To capture the uplift of the bearing, the elastic behaviour in the direction normal to the sliding surface is modified by assuming no-tension behaviour (Mazzoni et al. 2006).

As an example, the role of Coulomb friction on the seismic response is illustrated in Fig. 9 for a SDOF system with mass  $m = 10$  tons, elastic stiffness  $k = 10^3$  kN/m, and viscous damping  $\zeta = 5\%$  under the N–S horizontal component of the main shock of May 29th 2012 Emilia earthquake (see Fig. 4b). Figure 9a shows the response of the system with no friction ( $\mu = 0$ ). In this case viscous damping leads to oscillations with exponentially decreasing displacement amplitude. However, if friction damping is added the dynamic motion ceases with a resulting permanent displacement corresponding to static equilibrium. This is shown in Fig. 9b for the damped system with friction coefficient  $\mu = 0.20$ . The force is limited by the friction threshold  $F = \mu mg = 19.6$  kN, as shown by the force–displacement diagram depicted in Fig. 10.

**Fig. 8** Scheme of the beam-to-column joint with friction device modelled by using the flat slider bearing element available in the OpenSees library



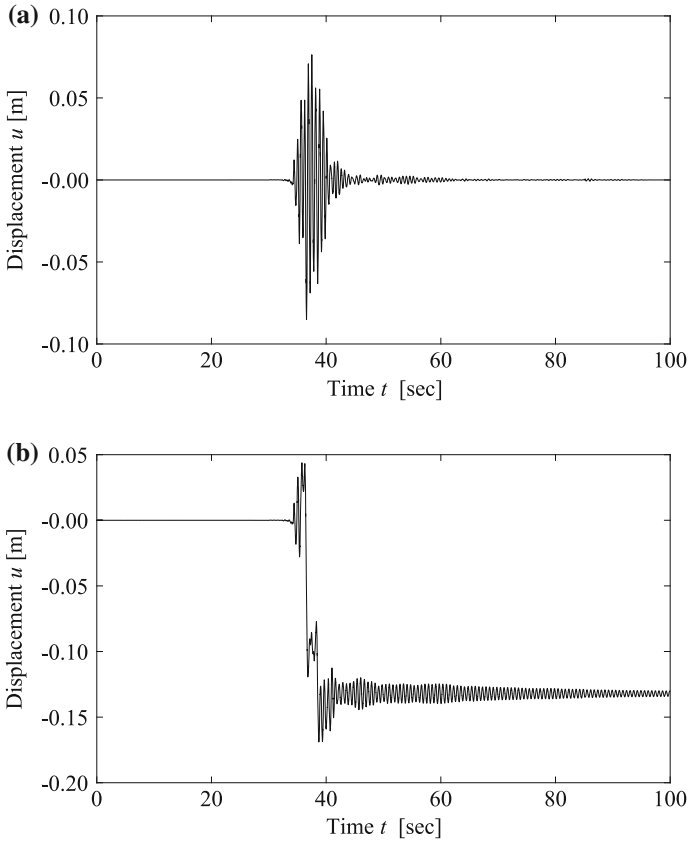


**Fig. 9** Displacement time-history of a SDOF system subjected to the N–S component of the May 29th Emilia earthquake: **a** viscous damping only ( $\xi = 5\%$ ); **b** viscous and friction damping ( $\mu = 0.20$ )

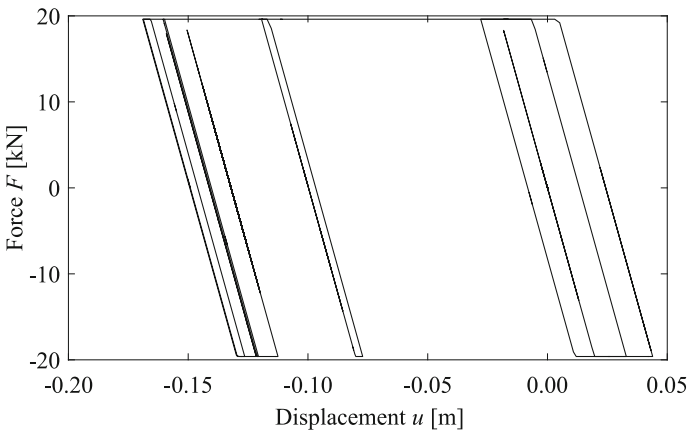


**Fig. 10** Force–displacement diagram of the SDOF system with viscous and friction damping (Fig. 9b)

## 4 Seismic response of one-storey precast buildings

The seismic response of one-storey precast frames is investigated by means of nonlinear time-history analyses considering a typical arrangement of precast building adopted in Italy and other countries (Biondini and Toniolo 2009; Liberatore et al. 2013; Belleri et al. 2015a, 2015b; Bournas et al. 2014; Magliulo et al. 2014; Casotto et al. 2015). It is shown how the lack of proper seismic details in the connection between columns and beams, where the transmission of shear forces is guaranteed only by friction, may lead to the collapse of the structure due to the loss of support of the main beam. The influence of the vertical component of the ground motion in triggering the structural collapse is also investigated.

### 4.1 Case study

The one-storey precast concrete frame with dry-friction joints between beam and columns shown in Fig. 11 is studied. Three different arrangements are considered, namely building types A, B, and C, with the main geometrical dimensions of the structure and size of the rectangular cross-sections of beams and columns listed in Table 1. The steel reinforcement of the column cross-sections is shown in Fig. 12. The geometrical dimensions have been selected in order to have natural vibration periods in the typical range of precast buildings in Italy ( $T = 0.71, 0.78, \text{ and } 0.95 \text{ s}$ , for building types A, B, and C, respectively). The amount of longitudinal and transversal reinforcement has been chosen to have a reinforcement ratio  $A_s/A_c > 1\%$  and a minimum stirrup spacing  $s = 300 \text{ mm}$ . A self-weight of the roof equal to  $2.4 \text{ kN/m}^2$  is assumed. The self-weight of the beams is computed by assuming a specific weight  $\gamma = 25 \text{ kN/m}^3$ .

Figure 13 shows the structural modelling and arrangement of the masses. A mass  $m_1$  is placed at top of the columns, corresponding to half of their self-weight. A series of five masses  $m_2$  are placed along the beam to account for the self-weight of both the beam and roof. Figure 13 shows also the force  $H(t)$  at the dry joint, and the horizontal displacements  $u_1$  and  $u_2$  of the column and the beam, respectively.

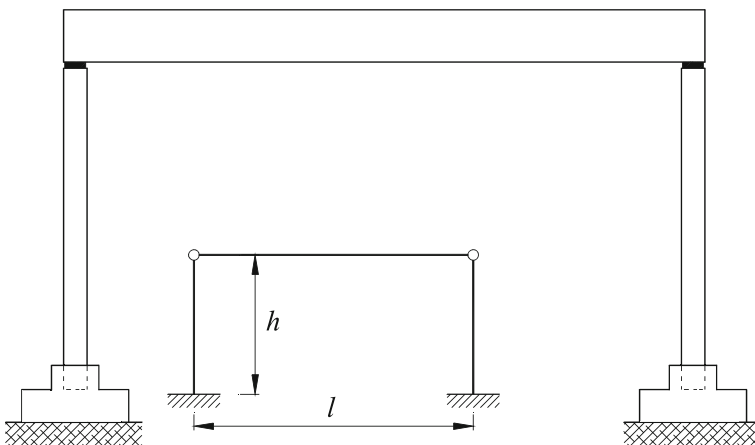


**Fig. 11** Precast frame building

**Table 1** Main dimensions of the structures and size of the cross-sections of columns and beams

Building	$h$ (m)	$l$ (m)	Column (mm)	Beam (mm)
A	5	12	300 × 450	250 × 600
B	6	17	300 × 600	250 × 850
C	7	22	450 × 600	300 × 900

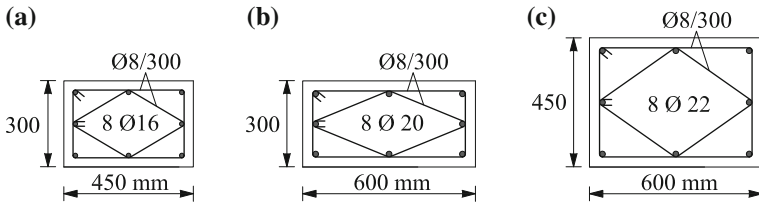


**Fig. 12** Cross-sections of the columns (mm)

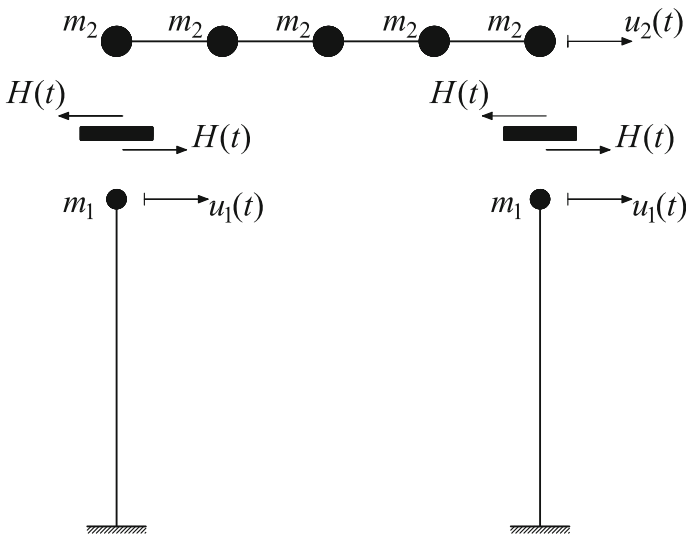


**Fig. 13** Structural modelling and arrangement of the masses

A nominal value of viscous damping  $\xi = 2\%$  is assumed. The nominal material strengths of concrete in compression and reinforcing steel are  $f_c = 48$  MPa and  $f_{sy} = 450$  MPa, respectively. Strain limits  $\epsilon_{cu} = 0.35\%$  and  $\epsilon_{su} = 7.5\%$  are assumed for unconfined concrete in compression and reinforcing steel, respectively. The effects of concrete confinement are taken into account as proposed by Mander et al. (1988). The columns are modelled using beam elements with distributed plasticity (Mazzoni et al. 2006). Elastic behaviour is assumed for the beams.

A neoprene pad is considered to be interposed between beam and columns. Regarding this assumption, it is worth noting that a different friction modelling may be required when

no rubber pad is present, as it is for many existing buildings with beam-to-column joints that are not connected with dowels (Liberatore et al. 2013).

The neoprene bearing is modelled by taking into account the elastic deformation of the rubber, as suggested by Magliulo et al. (2008). In particular, the shear stiffness  $K_t$ , normal stiffness  $K_n$ , and rotational stiffness  $K_\phi$  are computed as follows:

$$K_t = \frac{G_g A_g}{h_g} \tag{6}$$

$$K_n = \frac{E_g A_g}{h_g} \left( \frac{1 + 0.5\mu_c \cdot n_1^2}{1 - \mu_c^2} \right) \tag{7}$$

$$K_\phi = \frac{E_g I_g}{h_g} \left( \frac{1 + 0.1\mu_c \cdot n_1^2}{1 - \mu_c^2} \right) \tag{8}$$

where  $\mu_c$  is a coefficient related to neoprene hardness ( $\mu_c = 0.5$  for soft rubbers),  $n_1$  is the neoprene support shape coefficient, evaluated as indicated in the design recommendations CNR10018 (CNR 1999),  $E_g$ ,  $G_g$ ,  $A_g$ ,  $I_g$ , and  $h_g$  are, respectively, the Young modulus, shear modulus, area, inertia and thickness of the neoprene pad. The values of the mechanical parameters and geometrical dimensions assumed in the analyses are listed in Table 2.

The integration of the equation of motion is based on the Newmark method, assuming  $\beta = 0.25$  (constant acceleration) and time step  $\Delta t = 0.005$  s. The convergence criteria is based on an energy increment test, as discussed in Mazzoni et al. (2006). The solution algorithm is primary based on the Newton method. However, when highly nonlinear behaviour occurs, the algorithm switches to different strategies, such as Newton method with initial stiffness, Broyden method, and Newton method with line search.

### 4.2 Results of nonlinear time-history analysis

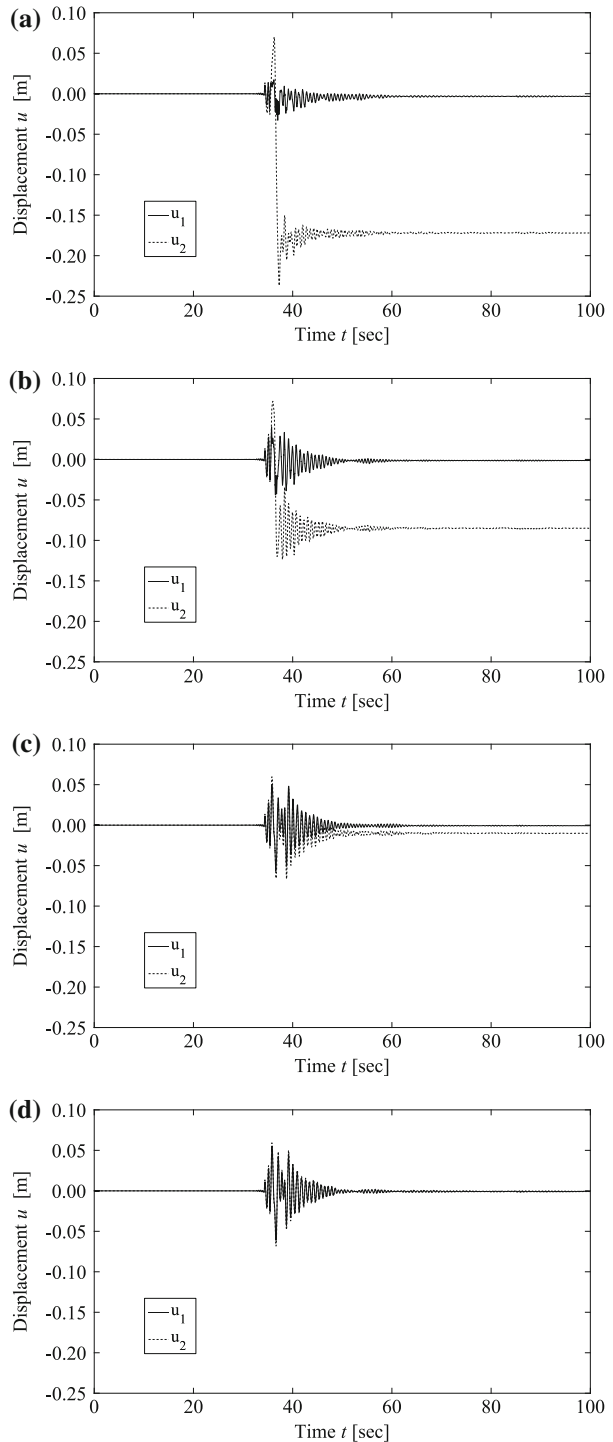
Nonlinear time-history analyses are carried out on the investigated frame buildings by assuming as seismic input the horizontal N–S component and the vertical component of the Emilia earthquake recorded on May 29th, 2012 (Fig. 4b, c). This was the event of the seismic sequence with the highest recorded vertical acceleration.

Figure 14 shows the displacement time-histories  $u_1 = u_1(t)$  of the column and  $u_2 = u_2(t)$  of building type A for different values of the friction coefficient  $\mu$  under the horizontal N–S component only. For moderate values of the friction coefficient, in the range  $0.10 \leq \mu \leq 0.30$ , a relative displacement between beam and columns occurs since the force slip threshold of the joint provided by friction is exceeded (Fig. 14a–c). The effectiveness of the connection is instead guaranteed for higher values of the friction coefficient, with no relative displacements between beam and columns as shown in Fig. 14d for  $\mu = 0.50$ . It is worth noting that the slip threshold is not constant during the motion due to the variation of the vertical force. This is highlighted in Fig. 15 which shows

**Table 2** Mechanical parameters and geometric dimensions of the neoprene pads (CNR 1999)

$E_g$ (kN/m <sup>2</sup> )	$G_g$ (kN/m <sup>2</sup> )	$A_g$ (m <sup>2</sup> )	$I_g$ (m <sup>4</sup> )	$h_g$ (mm)
2000	900	$0.10 \times 0.25$	$0.10 \times 0.25^3/12$	5

**Fig. 14** Displacement time-history of the column ( $u_1$ ) and the beam ( $u_2$ ) for different values of the friction coefficient  $\mu$ : **a**  $\mu = 0.10$ , **b**  $\mu = 0.20$ , **c**  $\mu = 0.30$ , **d**  $\mu = 0.50$



the diagrams of both horizontal force  $F$  (Fig. 15a) and normalized vertical force  $N/W_1$  (Fig. 15b) vs displacement  $u_2$ , where  $W_1 = W/2$  is half of the total seismic weight  $W$ . These diagrams exhibit a sudden shift in the hysteretic behaviour at about 38 s (see Fig. 14a) and a consequent residual displacement.

Experimental tests carried out by Magliulo et al. (2011) indicate a neoprene-concrete friction coefficient ranging from 0.09 to 0.13. A friction coefficient  $\mu = 0.10$  is hence assumed to investigate the role of the vertical component of the ground motion. Figure 16 shows the time-histories of the relative displacement  $\Delta = u_2 - u_1$  for the three types of building for two separate cases, without and with the simultaneous application of the vertical acceleration. It is noted that for building A the simultaneous application of the horizontal and vertical components of the ground acceleration leads to increased relative displacements (Fig. 16a). This result indicates, as expected, that the loss of support of the main beam is more likely to occur under significant vertical components of the ground motions. On the contrary, for buildings B and C the higher values of the relative displacement are achieved without the vertical component of the ground motion (Fig. 16b, c). Such result can be explained comparing the power spectral densities (Bendat and Piersol

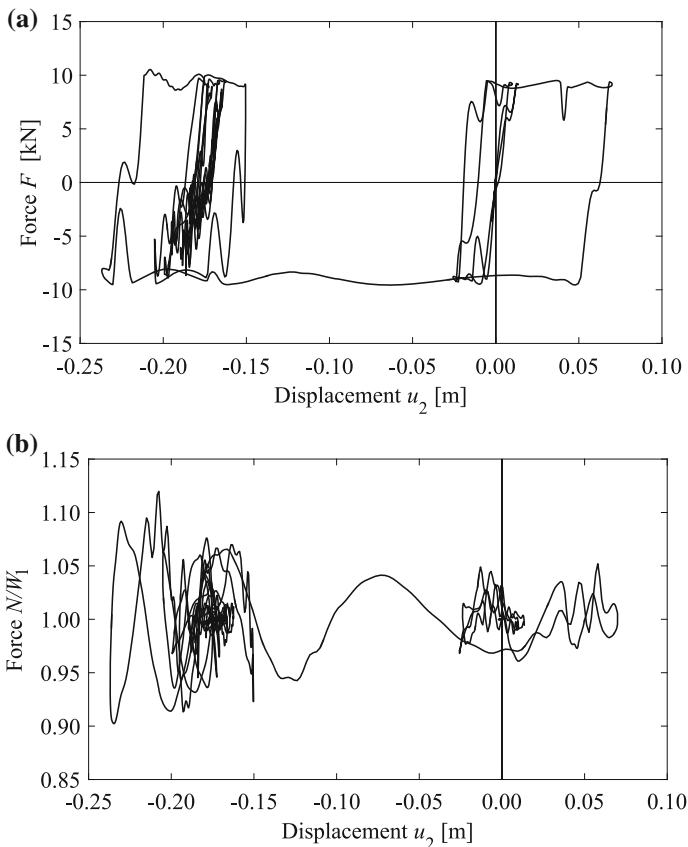


**Fig. 15** Force components vs. displacement  $u_2$  for building type A with friction coefficient  $\mu = 0.10$  under the horizontal component N–S of the Emilia earthquake recorded on May 29th, 2012: **a** Horizontal force  $F$ ; **b** Normalized vertical force  $N/W_1$  ( $W_1 = W/2$ )

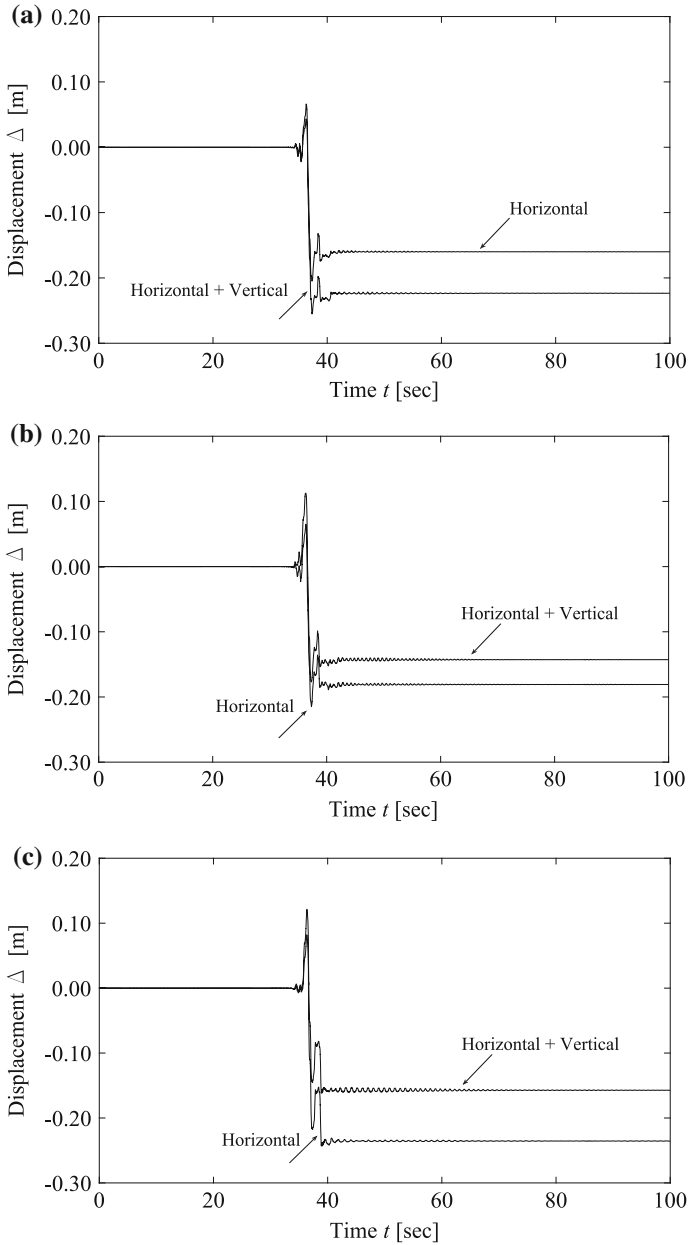


**Fig. 16** Relative displacement  $\Delta = u_2 - u_1$  for the three cases studied assuming a friction coefficient  $\mu = 0.1$  and the horizontal component N–S of the seismic event recorded on May 29th, 2012, with and without the vertical component: **a** Building A, **b** Building B, **c** Building C

1993) of the horizontal and vertical accelerograms with the natural vibration frequencies of the three buildings, respectively 2.11, 1.87, and 1.53 Hz for the horizontal component, and 3.79, 3.04, and 2.09 Hz for the vertical component. The comparison is shown in Fig. 17. It



is noted that the natural vibration frequencies in the vertical direction for building A and in the horizontal direction for building C are associated with the peak of the corresponding power spectral densities. The more flexible building A is hence more prone to suffer a loss of beam support if the vertical component of the ground motion is taken into account. In particular, under the resonance conditions the loss of support of the beam can occur also for low seismic intensities (Biondini et al. 2013b).

The results of the numerical simulations show that, for structural arrangements usually adopted in practice, high relative beam-to-column displacements may occur under earthquake conditions (up to 24 cm, see Fig. 16). The relative displacement has to be compared with the available bearing length to compute the residual bearing length. Large values of relative displacement may indicate an inadequate bearing strength of the support, leading to local rupture and possible consequent collapse or even to the fall of the beam out of its support. This has been the cause of many collapses occurred during the 2012 Emilia earthquakes. It is worth mentioning that in all the cases studied, the maximum relative displacement exceeded the nominal mean value of 10 cm (Fig. 16), that is suggested as limit state threshold in a first quick survey for stability assessment (Liberatore et al. 2013).

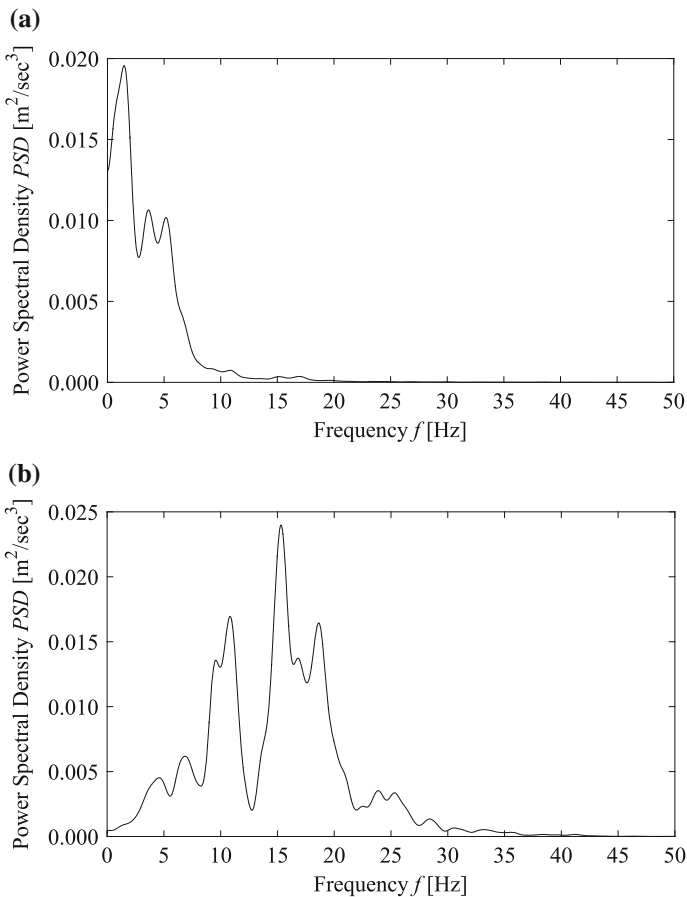


**Fig. 17** Power spectral densities of the horizontal and vertical components of the seismic motion recorded on May 29th, 2012. **a** N–S component **b** Z component

In conclusion, for existing buildings with dry-friction beam-to-column joints in seismic areas a proper modelling of the dry-friction joint behaviour is necessary to assess the building stability and check the need of proper strengthening interventions.

## 5 Conclusions

This paper presented a procedure for seismic assessment of precast buildings with beam-to-column dry connections, where the transmission of shear forces is guaranteed only by friction. Many industrial buildings in Italy are still characterized by this arrangement. Recent seismic events, including the Emilia earthquakes in 2012, emphasized the high vulnerability of these systems, since a significant number of failures has been observed due to the loss of support of the main beams. This type of failure has been one of the main reasons of the extensive damages and structural collapses that affected precast industrial buildings not designed for seismic action.

A proper modelling of the beam-to-column dry joint has been proposed, and a parametric study exploiting nonlinear dynamic analysis has been carried out for different buildings and different values of the dry friction coefficient. The results pointed out that small values of the friction coefficient, in the range 0.10–0.20 as indicated by the results of experimental tests carried out by Magliulo et al. (2011), may lead to a significant relative displacement between the beam and the column, which in turn may drive to the structural collapse due to the loss of support of the beam. In addition, it has been shown that this condition is more likely to occur under a relevant vertical component of the ground motion, particularly when the natural vibration frequency of the structural components in the vertical direction is close to the main frequencies of the seismic action. This highlights the importance of a proper modelling of the hysteretic behaviour of dry-friction joints for the seismic vulnerability assessment and design of retrofitting interventions for existing precast buildings in seismic areas.

For new precast buildings, a proper seismic design should include dowel connections between beams and columns. The involvement of cladding panels in the earthquake resisting system is also possible. In particular, the use of dissipative connections between the panels allows to calibrate the repartition of forces on the structural parts (frame and walls) and to keep in this way forces and displacements within allowable levels. More details can be found in Biondini et al. (2013a, 2017), Dal Lago et al. (2017) and Toniolo and Dal Lago (2017).

## References

- Artioli E, Battaglia R, Tralli A (2013) Effects of May 2012 Emilia earthquake on industrial buildings of early '900 on the Po river line. *Eng Struct* 56:1220–1233
- Babič A, Dolšek M (2016) Seismic fragility functions of industrial precast building classes. *Eng Struct* 118:357–370
- Belleri A, Brunesi E, Nascimbene R, Pagani M, Riva P (2015a) Seismic performance of precast industrial facilities following major earthquakes in the Italian territory. *J Perform Constr Facil* 29(5):04014135
- Belleri A, Torquati M, Riva P, Nascimbene R (2015b) Vulnerability assessment and retrofit solutions of precast industrial structures. *Earthq Struct* 8(3):801–820
- Bendat JS, Piersol AG (1993) *Engineering applications of correlation and spectral analysis*, 2nd edn. Wiley, New York

- Biondini F, Toniolo G (2009) Probabilistic calibration and experimental validation of the seismic design criteria for one-story concrete frames. *J Earthq Eng* 13(4):426–462
- Biondini F, Tsionis G, Toniolo G (2010) Capacity design and seismic performance of multi-storey precast structures. *Eur J Environ Civil Eng* 14(1):11–28
- Biondini F, Titi A, Toniolo G (2012) Pseudodynamic tests and numerical simulations on a full-scale prototype of a multi-story precast structure. In: Fifteen world conference on earthquake engineering (15th WCEE), Lisbon, Portugal, 24–28 September 2012
- Biondini F, Dal Lago B, Toniolo G (2013a) Role of wall panel connections on the seismic performance of precast structures. *Bull Earthq Eng* 11(4):1061–1081
- Biondini F, Titi A, Toniolo G (2013b) Prestazioni sismiche di strutture prefabbricate con connessioni travelpilastro ad attrito. In: Fifteen Italian conference on earthquake engineering (XV ANIDIS), Padua, Italy, 30 June–3 July 2013 (in Italian)
- Biondini F, Dal Lago B, Toniolo G (2017) Experimental tests on dissipative cladding connection systems of precast structures. In: Sixteen world conference on earthquake engineering (16th WCEE), Santiago, Chile, 9–13 January 2017
- Bournas DA, Negro P, Taucer F (2014) Performance of industrial buildings during the Emilia earthquakes in Northern Italy and recommendations for their strengthening. *Bull Earthq Eng* 12(5):2383–2404
- Braga F, Gigliotti R, Monti G, Morelli F, Nuti C, Salvatore W, Vanzi I (2014) Speedup of post earthquake community recovery: the case of precast industrial buildings after the Emilia 2012 earthquake. *Bull Earthq Eng* 12(5):2405–2418
- Casotto C, Silva V, Crowley H, Nascimbene R, Pinho R (2015) Seismic fragility of Italian RC precast industrial structures. *Eng Struct* 94(1):122–136
- Chopra AK (2007) Dynamics of structures: theory and application to earthquake engineering, 3rd edn. Prentice Hall, Englewood Cliffs
- CNR (1999) Apparecchi di appoggio per le costruzioni. Istruzioni per l'impiego (CNR 10018). Rome, Italy (in Italian)
- Colombo A, Negro P, Toniolo G (2014) The influence of claddings on the seismic response of precast structures: the Safeccladding project. In: Second European conference on earthquake engineering and seismology (2nd ECCES), Istanbul, Turkey, 25–29 August 2014
- Dal Lago B, Biondini F, Toniolo G (2017) Friction-based dissipative device for precast concrete panels. *Eng Struct* 147:356–371
- Faenza L, Michelini A (2010) Regression analysis of MCS intensity and ground motion parameters in Italy and its application in ShakeMap. *Geophys J Int* 180(3):1138–1152
- Faenza L, Michelini A (2011) Regression analysis of MCS intensity and ground motion spectral accelerations (SAs) in Italy. *Geophys J Int* 186(3):1415–1430
- Hong HK, Liu CS (2000) Coulomb friction oscillator: modelling and responses to harmonic loads and base excitations. *J Sound Vib* 229(5):1171–1192
- Iervolino I, De Luca F, Chioccarelli E (2012) Engineering seismic demand in the 2012 Emilia sequence: preliminary analysis and model compatibility assessment. *Ann Geophys* 55(4):639–645
- Kumar M, Whittaker AS, Constantinou MC (2015) Characterizing friction in sliding isolation bearings. *Earthq Eng Struct Dyn* 44(9):1409–1425
- Lauciani V, Faenza L, Michelini A (2012) ShakeMaps during the Emilia sequence. *Ann Geophys* 55(4):631–637
- Liberatore L, Sorrentino L, Liberatore D, Decanini LD (2013) Failure of industrial structures induced by the Emilia (Italy) 2012 earthquakes. *Eng Fail Anal* 34:629–647
- Magliulo G, Fabbrocino G, Manfredi G (2008) Seismic assessment of existing precast industrial buildings using static and dynamic nonlinear analyses. *Eng Struct* 30(9):2580–2588
- Magliulo G, Capozzi V, Fabbrocino G, Manfredi G (2011) Neoprene–concrete friction relationships for seismic assessment of existing precast buildings. *Eng Struct* 33(2):532–538
- Magliulo G, Ercolino M, Petrone C, Coppola O, Manfredi G (2014) The Emilia earthquake: seismic performance of precast reinforced concrete buildings. *Earthq Spectra* 30(2):891–912
- Mander JB, Priestley MJN, Park R (1988) Theoretical stress-strain model for confined concrete. *J Struct Eng* 114(8):1804–1826
- Manfredi G, Prota A, Verderame GM, De Luca F, Ricci P (2014) 2012 Emilia earthquake, Italy: reinforced concrete buildings response. *Bull Earthq Eng* 12(5):2275–2298
- Mazzoni S, McKenna F, Scott MH, Fenves GL, et al. (2006) Open system for earthquake engineering simulation (OpenSees). OpenSees command language manual. Pacific earthquake engineering research center (PEER), College of Engineering, University of California, Berkeley, CA, USA
- Negro P, Lamperti Tornaghi M (2017) Seismic response of precast structures with vertical cladding panels: the SAFECCLADDING experimental campaign. *Eng Struct* 132:205–228

- Negro P, Bournas DA, Molina FJ (2013) Pseudodynamic tests on a full-scale 3-storey precast concrete building: global response. *Eng Struct* 57:594–608
- Olgiasi M, Negro P, Bournas D (2011) Literature survey and identification of needs—part two: general survey and design procedures. In: Contribution of the Joint Research Centre. SAFECAST-Deliverable 1.2
- Rao SS (2011) *Mechanical vibrations*. Prentice Hall, Englewood Cliffs
- Toniolo G (2012) SAFECAST project: European research on seismic behaviour of the connections of precast structures. In: Fifteen world conference on earthquake engineering (15th WCEE), Lisbon, Portugal, 24–28 September 2012
- Toniolo G, Colombo A (2012) Precast concrete structures: the lessons learned from the L’Aquila earthquake. *Struct Concr* 13(2):73–83
- Toniolo G, Dal Lago B (2017) Conceptual design and full-scale experimentation of cladding panel connection systems of precast buildings. *Earthq Eng Struct Dyn*. <https://doi.org/10.1002/eqe.2918>